17. ASH LAYERS FROM DEEP SEA DRILLING PROJECT LEG 84: MIDDLE AMERICA TRENCH TRANSECT[1]

A. Pouclet and J. P. Cadet, Département des Sciences de la Terre, Université d'Orléans
K. Fujioka, Ocean Research Institute, University of Tokyo
and
J. Bourgois, Département de Géotectonique, Université Pierre et Marie Curie[2]

ABSTRACT

Three Leg 84 sites provided a good record of explosive volcanism onshore (in Central America). Ash layers and many ashy pods are interbedded in Recent to Oligocene strata. Evidence of the main periods of activity was noted in Recent to upper Pleistocene, Pliocene–Pleistocene, lower Pliocene to upper Miocene, lower Miocene, and upper Oligocene. Noticeable traces of older volcanism were found in upper Eocene strata.

The chemical analyses of glass shards show a dacitic to rhyolitic composition with a low to moderate calc-alkalinity. A preliminary distinction of samples in three geochemical groups according to their K_2O/SiO_2 contents is done to test a magmatic evolution. Comparisons are made with Leg 67 and on-land data.

INTRODUCTION

During Leg 84 the landward slope of the Middle America Trench off Guatemala was drilled (Fig. 1). At the sites where basement was penetrated, it was found to consist of ophiolitic rock (Aubouin, von Huene, et al., 1982) covered by sediments of the early Eocene (Sites 569, 570), the late Oligocene-early Miocene overlying Late Cretaceous (567), and the late Miocene (566, 568). The sites are distributed along a traverse roughly perpendicular to the margin (Fig. 2) and provide the opportunity to establish a chronology of airborne volcanic ashes interbedded within the sediments. The data of both Leg 66 north of Tehuantepec Ridge and of Leg 67 off Guatemala gave good records of explosive volcanism onshore because of the location of the sites close to volcanic sources and because of the direction of prevailing winds and marine currents.

ASH AT LEG 84 SITES

Drilling was done at five sites, but Site 567, at the base of the slope, and Site 566, 22 km upslope from the axis of the Trench (Fig. 2), were devoid of significant ash layers. At three sites good stratigraphic samples were recovered.

Site 569

Site 569 is located at a depth of 2770 m (27 km from the Trench axis and 125 km south of the coast of Guatemala). Ash layers are present in Pleistocene to upper Oligocene strata (Fig. 3). They are more numerous in the Pleistocene, where 17 thin (2 cm average) and fine-grained (fine silt generally) ash layers and many ash pods are interbedded in mud, and in the lower Miocene, where 29 ash beds can be counted. Colors range from very light gray to white (N8, N9) (in this case beds are rich in volcanic glass, 60–80%), to light gray olive (10Y 4/2), and olive-black (5Y 2/1) with marked amounts of quartz, alkaline feldspar, plagioclase, pyroxene, and amphibole. Upper Oligocene ashes are pale reddish purple (5NP 6/2) in Core 569A-2 and medium gray (N4) in Core 569A-7; these ashes are more clay-rich (Fig. 4). The oldest hemipelagic sediments of the Eocene (Core 569A-9) contain some traces of volcanic activities—fragments of glass, quartz, and feldspar disseminated in bioturbated mudstone; but no ash layers were recorded because of poor core recovery.

Site 568

Site 568 is located at a depth of 2031 m on the upper slope, about 45 km from the Trench axis. Recent to upper Pleistocene muds contain 17 distinct thin layers of ash, as at Site 569, and numerous ashy mottles and pumice clasts; these occur mainly in the upper part of the section. Colors vary from light gray (N7) to medium bluish gray (5B 5/1) and olive black (5Y 2/1) to pale olive (10Y 4/2). Grain size ranges from very fine silt (most commonly) to silt.

Upper Miocene to lower Miocene–upper Oligocene mudstones, above Core 568-41, contain numerous (30) ash layers as well as numerous ashy mottles and pumice clasts, mainly in middle Miocene strata. Some beds are rich (5–7%) in biotite, for example, Samples 568-7-1, 139–141 cm or 568-29-1, 59–61 cm. Glass percentage decreases downsection (25–35% in Oligocene) because of alteration.

Site 570

Site 570 is located on the edge of a small bench in the upper slope, 40 km north of the Trench axis. Ash layers
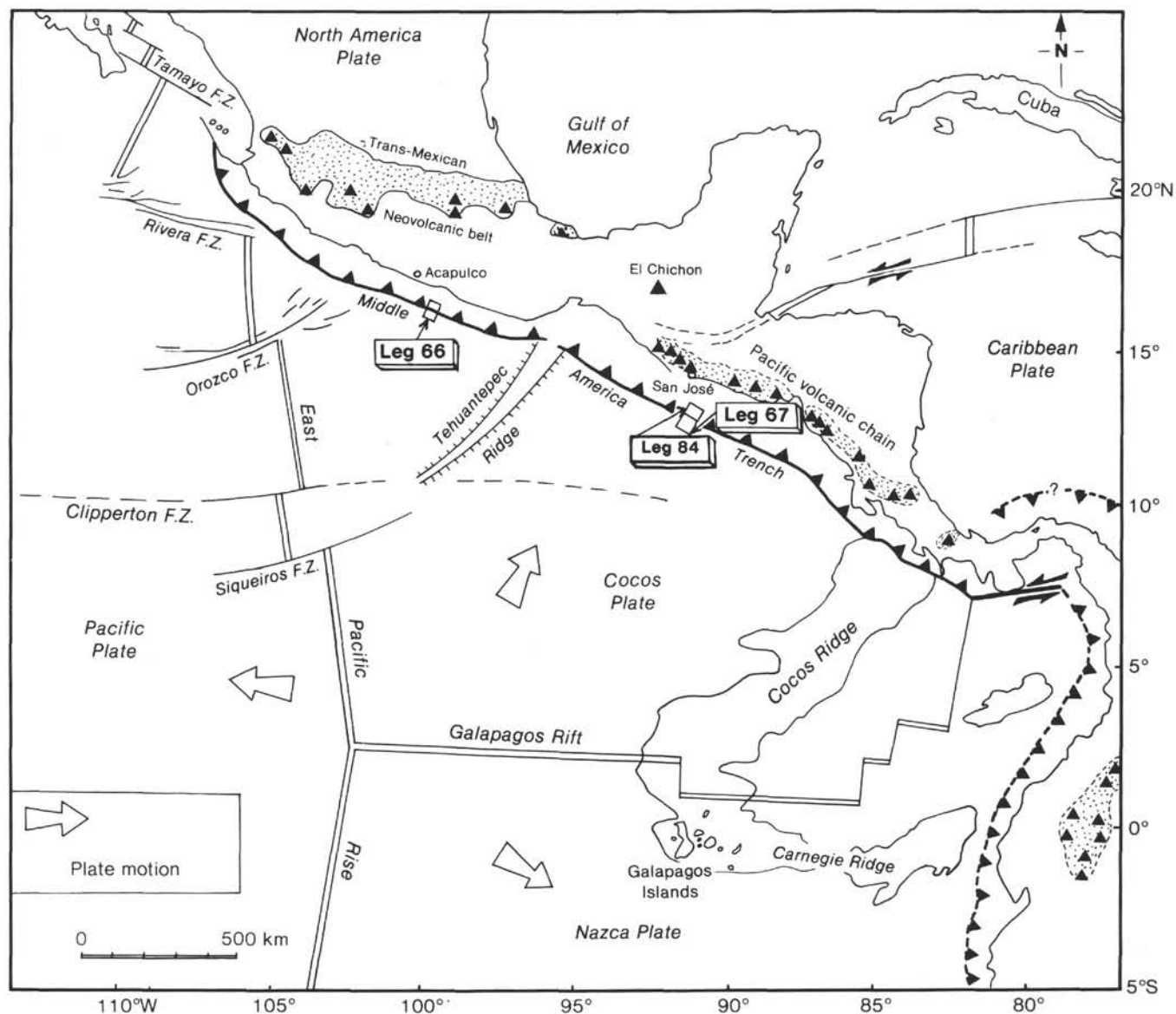
Figure 1. Geological setting of Legs 84, 66, and 67. Eastern Cocos Plate boundary after Lonsdale and Klitgord (1978).

occur mainly in Pleistocene mud (10 counted). They vary in color from very light gray (N8) (the richest in volcanic glass, up to 90%) to moderate olive brown (5Y 4/4) and olive gray (5Y 3/2). Thickness of ash layers is slightly greater, reflecting the site's proximity to land, and graded beds containing quartz and feldspars in amounts up to 20% occur. In upper Miocene sediment, ash beds are scarce (3 counted); they are medium light gray (N6) and fine-grained.

GEOCHEMISTRY

METHOD

Nineteen ash layers were sampled at Sites 569, 568, and 570 from the Trench upper slope to the foot of the continental talus. Their age ranges from late Oligocene to Recent. Figure 5 gives the distribution of analyzed samples. Fifty-six specimens of glass shards were analyzed using a JEOL EPMA (JCXA 733) electron-probe microanalyzer at the Ocean Research Institute, Tokyo University. The analyses were per-

formed using a 15-kV accelerating voltage, and 20-μm average defocused beam diameter, 10-s count time, with the elements ordered as follows: Na, K, Si, Fe, Mg, Al, Ti, Mn, Ca, Ni, and Cr.

Chemical Composition of Glass Shards

SiO_2 contents range from 58.14 to 73.30% (Table 1); most samples have acidic compositions. The analyses total between 91 to 95%. This important deficit is a well-known problem in ash analysis. As the selected samples are devoid of apparent alteration, this deficit could be accounted for by hydration of glass and analytical error. Because the iron content is very low, oxidation of iron cannot be responsible for the low totals. It is difficult to analyze glasses with a microprobe owing to the volatility of elements such as Na and K in this kind of material. However, a significant drift only appears after a count time exceeding 30 s. In order to avoid this problem, the most volatile elements were analyzed first with short
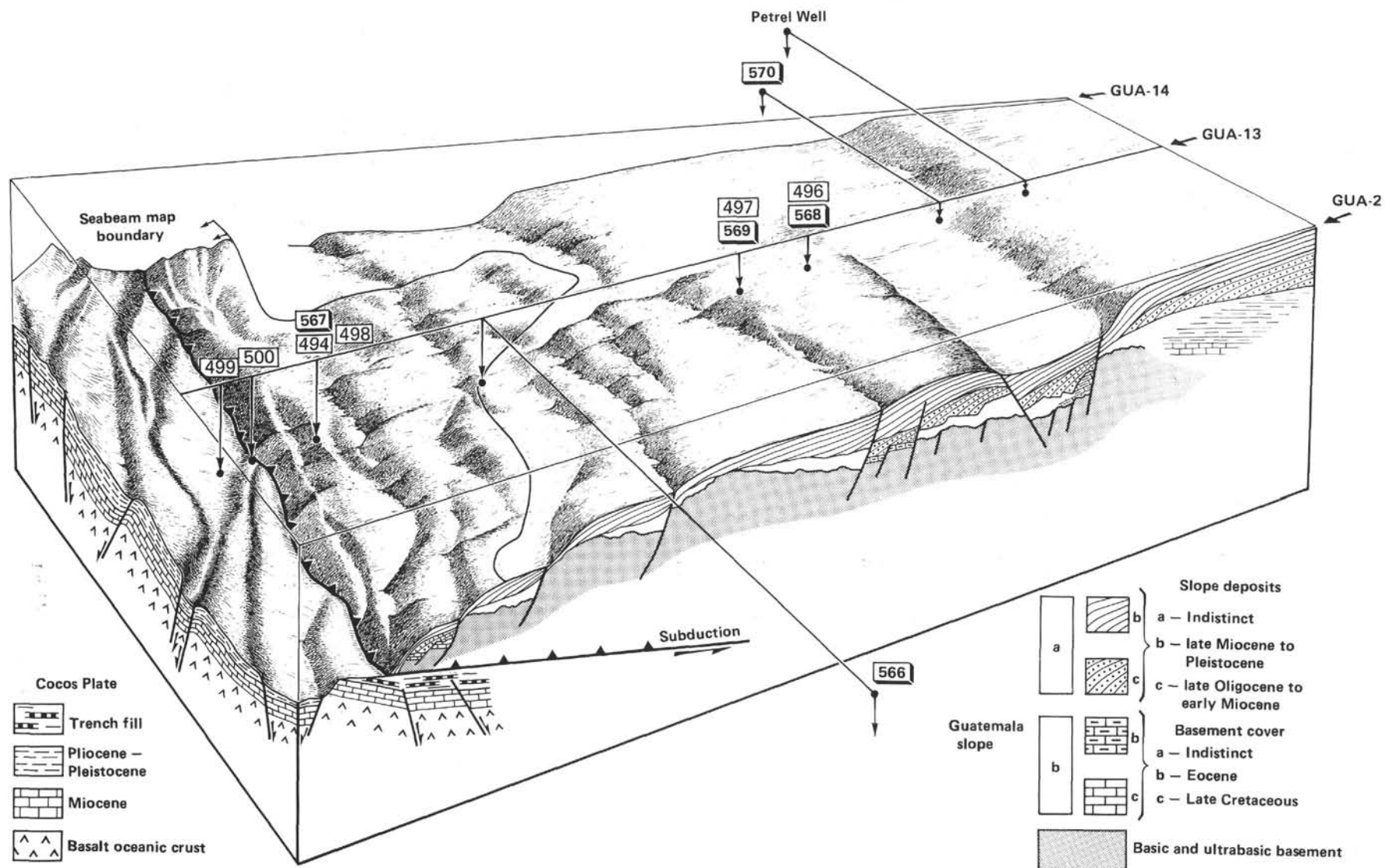
Figure 2. Block diagram showing the position of Guatemalan Leg 84 and some Leg 67 sites on the landward wall of the Middle America Trench (after Aubouin, von Huene, et al., 1982).
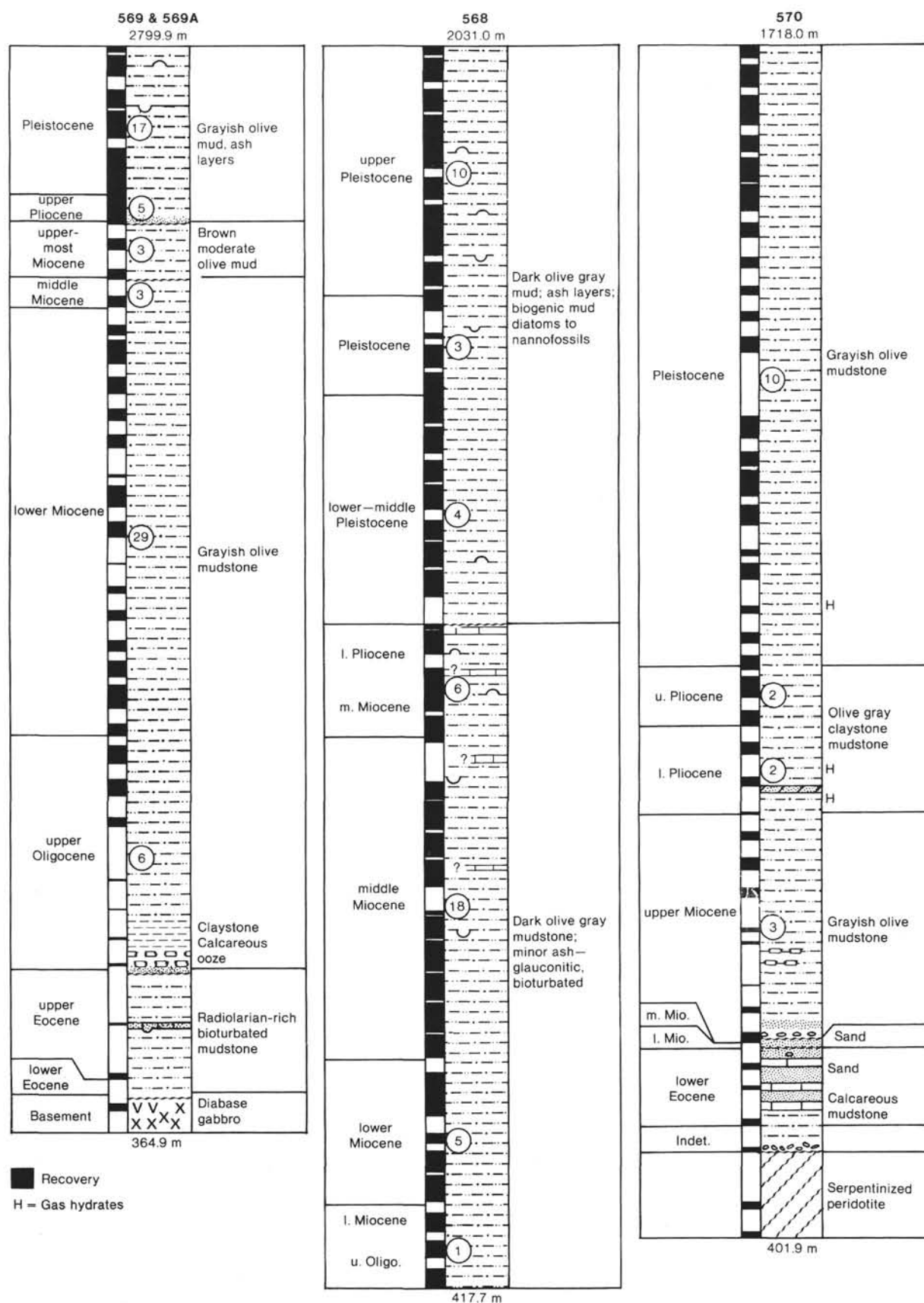
Figure 3. Holes 569, 569A, 568, and 570 simplified stratigraphic columns; circled numbers show the number and position of ash layers in the recovered sediment sections.

Age	Group	Sample (core-section, interval in cm)	Volcanic glass (%)	Number of analyses	Clay (%)	Quartz (%)	Feldspar (%)	Heavy minerals (%)	Fossils (%)
		Holes 569 and 569A	0 100						
lower Pleist.— upper Pliocene	3	7-2, 139—141		3					
middle Miocene	5	10,CC (16—18)		7					
lower Miocene	6	11-1, 78—80		4					
upper Oligocene	7	A7-1, 83—85		2					
		Hole 568							
Recent	1	5-5, 38—40		2				Hg	
		5-7, 20—22		2				Hb	
upper Pleistocene	2	10-1, 97—99		5				Hg	
lower Pleist.— upper Pliocene	3	20-7, 7—9		3				Hg	
lower Pliocene	4	23-2, 90—92		3					
middle Miocene	5	27-4, 88—90		1				Hg	
		29-1, 59—61		1				Py	
		29-1, 138—139		4					
		35-6, 76—78		7					
		37-4, 39—41		1					
lower Miocene	6	38-1, 120—122		4					
		Hole 570							
Present	1	2-1, 141—143		3					
		2-3, 108—110		2				Hg-b	
lower Pleist.— upper Pliocene	3	23-2, 74—76		1				Hb	
upper Miocene	5	32-4, 120—122		1					

Figure 4. Result of smear slide analysis of the electron-probe micro-analyzed samples; distribution and number of analyses of volcanic glass shards. (H = hornblende, g = green, b = brown, Py = pyrite).

Table 1. Selected microprobe analyses of glass shards (%).

Sample (interval in cm)	568-5-5, 38–40 [1]		568-5-7, 20–22 [1]		568-10-1, 97–99 [2]		568-20-7, 7–9 [3]		568-22-3, 90–92 [4]			568-27-4, 88–90 [5]	568-29-1, 59–61 [5]	568-29-1, 138–139 [5]				568-35-6, 76–78 [5]	
Petrographic type	Dc	Dc	Rh	Rh	Rd	Rh	Rd	Dc	Dc	Dc	An	Rh	Dc	Dc	Rd	Dc	Rd	Rd
Magmatic group	C	C	B	B	A	A	B	AB	C	C	C	C	B	B	C	C	C	C
Analysis number	131	135	14	15	146	149	142	143	136	138	140	31	29	24	25	26	92	93
SiO$_2$	66.48	67.45	73.30	73.25	70.76	72.05	71.16	68.49	69.92	65.70	58.14	72.59	68.89	68.85	70.26	69.98	71.96	70.77
TiO$_2$	0.14	0.10	0.07	0.10	0.18	0.21	0.20	0.18	0.13	0.40	0.99	0.17	0.17	0.21	0.13	0.14	0.02	0.03
Al$_2$O$_3$	14.04	13.86	12.11	12.19	12.52	12.66	12.11	14.92	13.47	14.11	15.59	11.79	13.35	13.98	12.82	12.65	12.68	12.58
ΣFeO	1.57	1.51	0.53	0.55	1.09	1.11	1.14	0.81	0.91	2.51	6.53	0.83	0.88	0.98	0.69	0.66	0.84	0.93
MnO	0.06	0.06	0.08	0.05	0.15	0.07	0.02	0.05	0.08	0.12	0.16	0.06	0.07	0.07	0.09	0.08	0.02	0.10
MgO	0.22	0.19	0.08	0.07	0.23	0.25	0.18	0.14	0.14	0.47	1.91	0.13	0.22	0.24	0.12	0.11	0.04	0.03
CaO	1.09	1.00	0.59	0.61	1.34	1.30	0.90	2.31	0.49	1.35	4.13	0.61	0.89	0.69	0.42	0.38	0.56	0.56
Na$_2$O	3.87	3.52	3.88	3.84	3.54	3.79	3.47	4.39	4.22	3.88	4.24	3.12	3.44	4.68	4.10	3.97	3.61	2.99
K$_2$O	3.38	3.27	3.36	3.46	1.93	1.95	2.86	2.15	3.27	3.58	2.54	3.79	3.05	2.67	3.64	3.29	3.66	4.24
NiO	0.02	0.04	—	—	—	—	0.02	tr	—	—	—	—	0.01	—	—	0.02	0.01	—
Cr$_2$O$_3$	—	—	—	0.02	—	—	0.01	0.01	0.01	0.03	—	0.01	0.01	0.04	0.01	—	—	—
Total	90.87	91.00	94.00	94.14	91.74	93.39	92.07	93.45	92.64	92.15	94.23	93.10	90.98	92.41	92.28	91.28	93.13	92.23

Note: Chronostratigraphic group is indicated in brackets below sample number: 1 = Recent, 2 = upper Pleistocene, 3 = lower Pleistocene-upper Pliocene, 4 = lower Pliocene, 5 = middle Miocene, 6 = lower Miocene, and 7 = upper Oligocene. Magmatic groups are A = low K, B = medium K, C = high K; petrographic types are Bs = basalt, An = andesite, Dc = dacite, Rd = rhyodacite, and Rh = rhyolite. Total Fe as FeO; — = not determined; tr = trace.
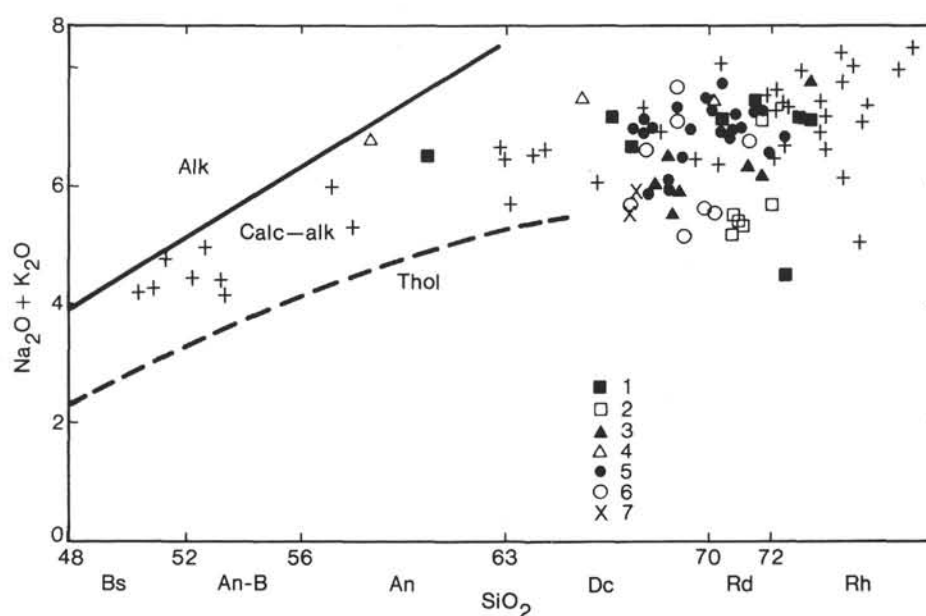

Figure 5. (Na$_2$O + K$_2$O)/SiO$_2$ diagram (chronostratigraphic groups: 1 = Recent; 2 = upper Pleistocene; 3 = lower Pleistocene–upper Pliocene; 4 = lower Pliocene; 5 = middle Miocene; 6 = lower Miocene; 7 = upper Oligocene; + = on-land tephras analyses for comparison (see references in the text). Alk/calc = alkaline/subalkaline lavas boundary (Irvine and Baragar, 1971). Calc-alk/thol = calc–alkaline/tholeiitic lavas boundary (Kuno, 1968). Petrographic identifications are Bs = basalt; An-B = basalt andesite; An = andesite; Dc = dacite; Rd = rhyodacite; Rh = rhyolite. SiO$_2$ typological boundaries are defined by Pecerillo and Taylor (1976) and are slightly modified for Rd, as in Cadet et al., 1982.

count times and a defocused beam. In agreement with several authors (cf., Cadet et al., 1981 and 1982), we suggest that hydration explains the greatest part of the analytical deficit. Because the deficit is independent of sample age, the hydration must have occurred at the time of deposition. Analysis of row data and data corrected by recalculating to 100%, like a water-free analysis, have been plotted on the same SiO$_2$/alkaline diagram (not shown). It appears that the corresponding points in the two groups are linked by parallel segments with very few exceptions. Even the proportion of the analyzed elements like the alkaline elements which are the most sensitive to alteration, is not perceptibly modified by the hydration (analytical deficit). In the following discussion, we use the row data from the 56 analyses.

Magmatic Characterization

Analyses are distributed in chronostratigraphic groups corresponding to the following main periods of volcanic activity: 1 = Recent, 2 = upper Pleistocene, 3 = lower Pleistocene–upper Pliocene, 4 = lower Pliocene, 5 = middle Miocene, 6 = lower Miocene, and 7 = upper Oligocene.

On the SiO$_2$-total alkaline diagram (Fig. 5), points appear scattered within the calc–alkalkine field, near the boundary of the tholeiitic field. According to the nomen-

Table 1. (Continued.)

568-37-4, 37-41 [5]	568-38-1, 120-122 [6]		569-7-2, 139-141 [3]	569-10,CC (16-18) [5]		569-11-1, 78-80 [6]		569-7-1, 83-85 [7]		570-2-1, 141-143 [1]	570-2-3, 108-110 [1]		570-23-2, 74 [3]	570-34-2, 120-122 [5]
Rh	Dc	Rd	Dc	Dc	Dc	Rd	Dc	Dc	Dc	Rd	Rd	An	Rh	Dc
C	A	A	A	C	A	B	C	A	A	B	B	B	C	C
98	34	102	46	54	83	59	77	70	72	13	10	121	8	111
72.02	67.22	70.13	68.61	67.52	68.56	71.24	69.82	67.24	67.42	71.55	70.21	60.26	73.26	67.59
0.24	0.42	0.30	0.29	0.37	0.24	0.09	0.08	0.33	0.33	0.11	0.10	0.58	0.08	0.17
11.65	13.94	13.06	13.87	13.22	13.80	11.97	13.35	14.31	13.73	12.36	12.11	15.15	12.33	13.80
1.05	1.98	1.45	2.15	1.57	2.12	0.91	1.07	1.79	1.80	0.66	0.79	4.39	0.65	1.61
0.02	0.06	0.03	0.05	0.10	0.08	0.05	0.11	0.07	0.12	0.08	0.14	0.19	0.08	0.05
0.15	0.59	0.38	0.47	0.34	0.46	0.12	0.15	0.54	0.56	0.07	0.17	1.85	0.04	0.22
0.83	2.22	1.69	2.06	1.22	2.12	0.56	0.84	2.20	2.01	0.36	0.42	2.67	0.19	1.04
2.84	3.99	3.65	3.82	3.86	4.03	3.68	3.67	3.80	3.84	4.22	3.97	4.35	2.99	3.70
3.75	1.74	2.00	2.09	3.20	2.06	3.15	3.59	1.90	2.07	3.22	3.24	2.20	4.87	3.37
—	—	—	0.03	tr	—	tr	—	0.05	—	0.06	—	—	0.02	0.04
0.01	0.01	—	—	0.01	—	—	—	—	—	—	—	—	—	—
92.56	92.17	92.69	93.44	91.41	93.47	91.77	92.68	92.23	91.88	92.69	91.15	91.64	94.51	91.59

clature of calc–alkaline lavas on SiO_2/K_2O diagrams (Fig. 6), we recorded 2 andesitic, 28 dacitic, 29 rhyodacitic, and 7 rhyolitic compositions.

As these data come from the same sampling and the same analysis series, their diversity reflects differences in volcanic source. Positive correlation of alkalis with SiO_2 is generally linked to magmatic differentiation in calc–alkaline trends; the scatter perpendicular to this direction, following a negative correlation, is larger than the sampling variation (glass heterogeneity) and analytical drift. This spread shows the existence of several magmatic trends with different alkalinity, as in Legs 66 and 67 (Cadet et al., 1981 and 1982). Because potassium is classically the element used in the distinction of calc–alkaline lines, we separated the data into three groups— A, B, and C—on the SiO_2/K_2O diagram (Fig. 6), following limits parallel to differentiation trends in order to detect a possibie evolution. To test this empiric subdivision, we performed a discriminant calculation—using MAHAL 3 (a computer program of Romeder, 1973), considering all the elements of the chemical analyses of the three groups; the calculation confirms the good sorting of over 80% of the samples in these groups. The first discriminant function includes as first significant

variable K_2O, then CaO, Na_2O, and Al_2O_3; the subdivision of groups is a distinction between calc–alkaline series. The first sorting using K_2O and SiO_2 in raw data (Fig. 6) can be considered satisfactory.

Chronological Evolution

The distinction of the products of more or less potassic lines or series eliminates the effect of differentiation and allows the chronological evolution of ash compositions to be plotted on a simple diagram: time/K_2O (Fig. 7). In this diagram, the K_2O content is considered as a parameter including SiO_2 (superposition of the groups).

In the Oligocene, dacites with a low potassic content appear. All three series appear in the lower Miocene as dacites and rhyodacites. They are found again in middle Miocene with highly potassic rhyolites. A single C-type, upper Miocene dacite sample has been analyzed. For the lower Pliocene, the sampling is limited to highly potassic andesites and dacites. The Pliocene-Pleistocene displays dacites, rhyodacites, and rhyolites from the three groups. Only low-potassic rhyodacites and rhyolites of group A have been analyzed for upper Pleistocene strata, but the other types do exist (cf., Leg 67, Cadet et al., 1982). Recent ash layers include moderately potassic an-
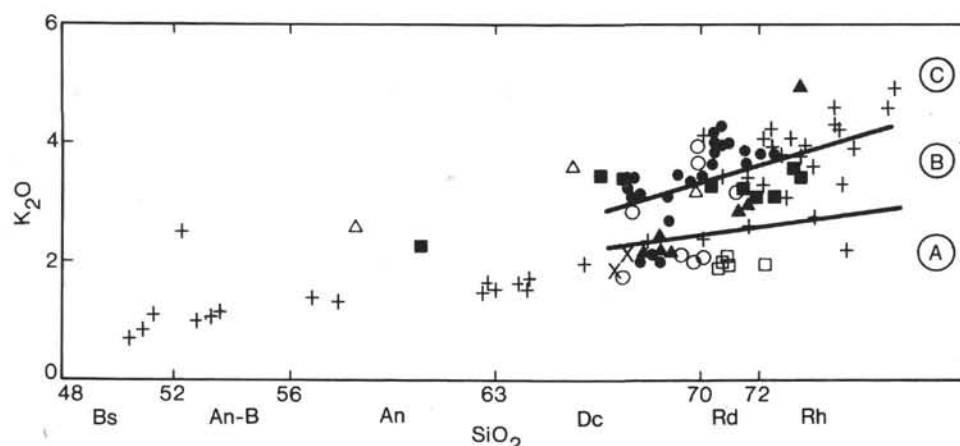

Figure 6. K_2O/SiO_2 diagram (for an explanation of symbols denoting chronostratigraphic groups and petrographic identifications, see Fig. 5). Magmatic groups are A = low K; B = medium K; and C = high K.
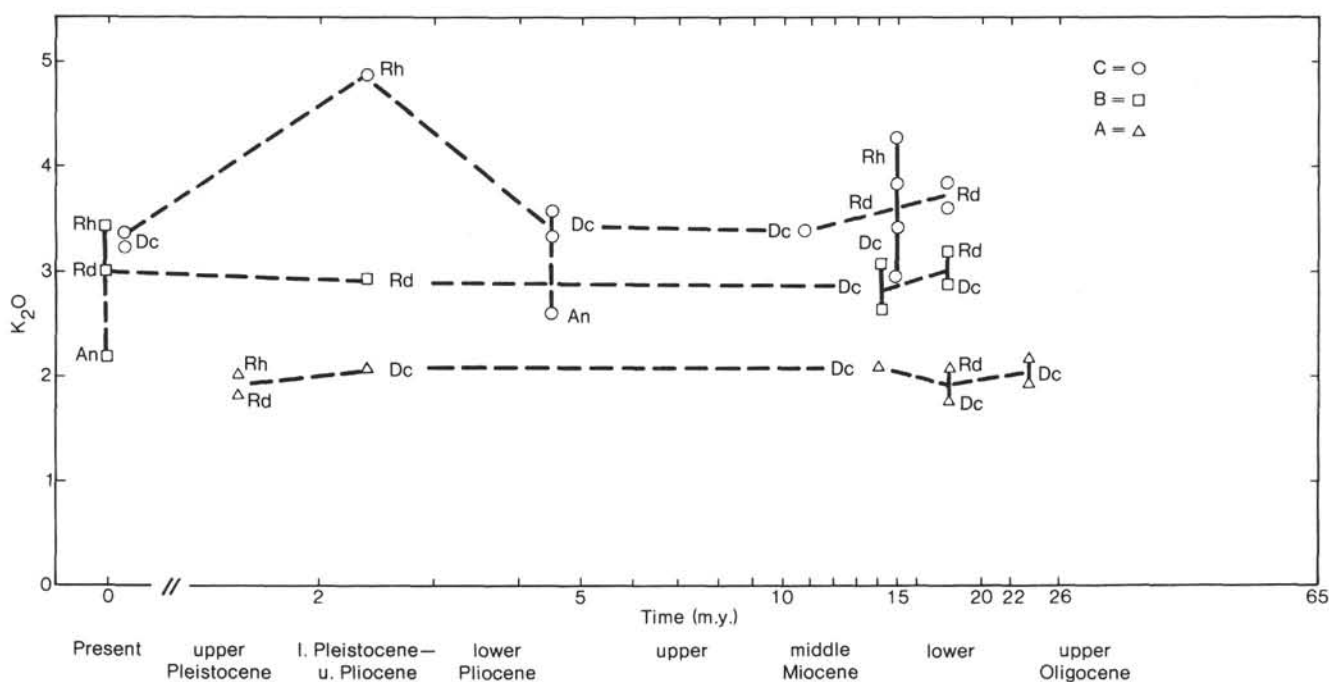
Figure 7. K₂O/time diagram. Potassic groups: A = low K; B = medium K; and C = high K. For petrographic identifications (An, Dc, etc.) see Figure 5.

desitic to rhyolitic glasses and a few highly potassic dacites.

A preliminary history of explosive volcanism of Central America since the Oligocene can be established in spite of insufficient sampling, taking into account the recording and the repartition of ash layers (i.e., loss of ash layers through alteration or erosional hiatuses). On the basis of two analyses, the first low potassic pulse appeared during the late Oligocene. A highly diversified magmatism developed during the early Miocene. This diversity remained in successive phases of activity: during the early Pliocene (preponderance of the highly potassic type), Pliocene–Pleistocene, and late Pleistocene. Only the moderate and high potassic series are represented in Recent sediments.

Comparison with Leg 67

Leg 67 includes 86 analyses of glasses sampled at four sites on the oceanic plates and the Trench lower slope (Cadet et al., 1982). The samples were analyzed using the BRGM-CNRS Camebax electron-probe microanalyzer in Orléans (France). Two sites, 496 and 497, were very close to Leg 84 at Sites 568 and 569; thus comparisons can be made on the same ash layers.

A shift in Leg 84 data, reflecting analytical conditions, was observed, with compositions systematically more alkaline and less siliceous (roughly +0.5 K₂O and −2 SiO₂) than those obtained for Leg 67 materials. Consequently, there is a displacement of AB and BC limits on the SiO₂/K₂O diagram used in the Leg 67 chapter (Cadet et al., 1982). However, taking into account this analytical shift, data from the two legs can be combined.

Upper Oligocene strata was not reached in Leg 67. Lower Miocene A-group glasses (low potassium content)

found at Site 496 have the same composition as those at Site 568. B and C products are located at Site 569 but, as it seems, in a higher stratigraphic level of the lower Miocene. All compositions of the middle Miocene appear at the same Site 496. These data tend toward a diversification of lines from the beginning of the Miocene to the middle Miocene, a period of intense activity. Later, the existence of all these series in Leg 84 is supported by Leg 67 samples: line A at lower Pliocene at Site 497, line C at the Pliocene–Pleistocene at the same site, line C equally (abundant) at upper Pleistocene at Site 496. Conversely, line A, limited to Pliocene-Pleistocene on Leg 67, reaches up to upper Pleistocene at Site 568.

Comparison with On-Land Volcanism

The deep-sea volcanic glasses studied here were originally explosive shards carried by winds from on-land volcanoes. In the area in question, the predominant winds are westerlies, as the El Chichon eruption clearly demonstrates (Robock and Matson, 1983). Thus in the north equatorial zone, the eastern Pacific mainly receives ashes from Guatemala, El Salvador, Costa Rica, and possibly southern Mexico. The eolian Central American origin of equatorial Pacific recent submarine ashes was geochemically verified by Boyles et al (1973). The silty size of shards and the presence of micropumice can correspond to eolian transportation exceeding distances of 100 km (Carey and Sigurdsson, 1980). There are no palagonitized glasses and no trace of submarine volcanism in the drilling area. Hot spots in the region are located farther southwest on Cocos Ridge (Lonsdale and Klitgord, 1978).

Comparison with on-land volcanism is limited by the scarcity of analyses of terrestrial glasses relative to analyses of lavas. Glassy materials are often, but not always,

richer in alkalis than corresponding whole rocks. As a rule, rhyolitic glasses correspond to dacitic lavas, dacitic glasses to andesitic lavas, and so on.

On an AFM diagram (Fig. 8), glasses from Legs 67 and 84 are distributed in the "T sector" are of middle America Tertiary and Quaternary lavas of Woodruff et al. (1979). Intermediate to basic compositions are located in the FeO-rich part where analyses of on-land glasses and vitreous inclusions plot "G sector"; see Cadet et al., 1982).

$SiO_2/(Na_2O + K_2O)$ and SiO_2/K_2O diagrams (Figs. 5 and 6) also show a selection of rhyolitic ash analyses from Guatemala and Columbia–Equador (Drexler et al., 1980) together with lava and glass compositions of Guatemala dacites and dacitic andesites (Rose, 1972a and b; Rose et al., 1978 and 1981; Bardintzeff et al., 1980). Acidic on-land samples are mainly located in moderately alkaline and potassic composition zones (groups B and C). Santiaguito dacitic glasses appear to have a low potassic content, but if statistical analyses takes into account all elements, these glasses are closer to the C group (Cadet et al., 1982). Basic lavas also have a low potassic content, but their glassy parts correspond to the C group.

In comparison, Columbia–Equador lavas have a higher potassic content than have Central America lavas, and so have South American volcanic materials, which clearly show a more calc-alkaline composition. However, some Columbia–Equador submarine glass samples of Leg 70, Galapagos (Schmincke, 1983), show a moderate alkalinity.

Tentative correlation of Recent deep-sea ash layers with Central American explosive deposits has been made using trace element data (INAA) on whole rock samples (Rose et al., 1982) or using principal component analysis with major elements composition (Cadet et al., 1982): Piños Altos and Los Chocoyos Quaternary tephra units of Guatemala correlate with Site 496 ash layers. Whole rock sample trace element correlation seems to be accurate. Major elements submarine glass chemistry may indicate an analytical analogy with on-land tephra, but the number of analyses is too low for a good statistical correlation.

CONCLUSIONS

1. *Initiation of volcanism.* The interbedding of ash layers in upper Oligocene mudstones recovered during Leg 84 allows the recording of a typical calc–alkaline volcanism of this age. This discovery may indicate that subduction had already begun in the Middle America Trench. There is evidence of an older volcanism during the late Eocene, offshore (Leg 84, Hole 569A) and on-land through middle Eocene andesitic flows in Costa Ri-
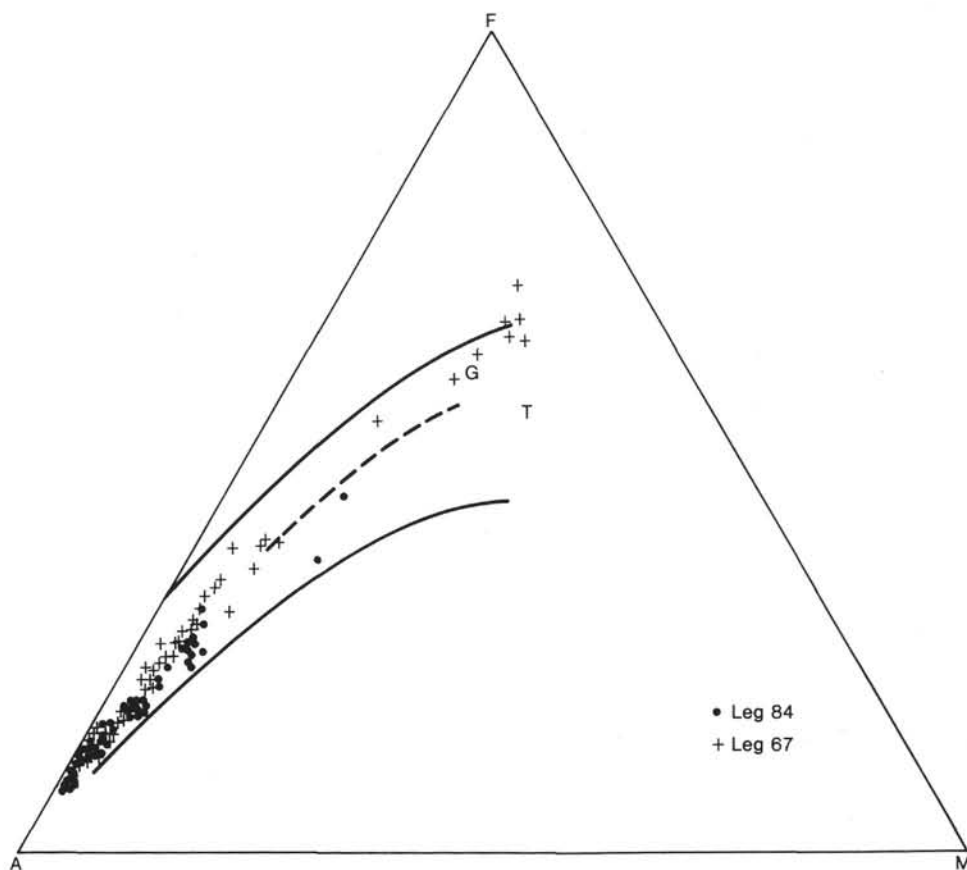

Figure 8. AFM diagram. Leg 67 (small crosses) and Leg 84 (black dots) glass analyses. T = Central America volcanic rocks area; G = on-land tephras and glassy magmatic inclusions analysis sector.

ca (Bellon and Tournon, 1978). Up to now this is the oldest known calc-alkaline volcanism in Central America, but its geodynamic meaning is not yet clear.

2. *Magmatic evolution.* At first, the magmatism seems to have a low-K_2O character according to a few preliminary analyses; from the beginning of early Miocene, it diversifies into calc-alkaline potassic-differentiated lavas. If the hypothesis of a relationship between K_2O content of primary magma and the dip of the Benioff zone (thus of depth of magma genesis) is followed (e.g., Keith, 1982), we can infer a correspondence of high subduction activity with the different periods of volcanism mainly during early-middle Miocene and late Pliocene-Pleistocene. However, because the analyzed samples are acid glasses, it may be emphasized that the differentiated lavas maintained the more or less potassic character of their different lines following crystal fractionation conditions. At present, the volcanism has a medium to high potassic content. Indeed, the dip of the subduction plate (according to Molnar and Sykes, 1969) is steeper off Guatemala than it is to the northeast (South Mexico) and southeast (Panama). But the K_2O content – Benioff dip relationship is still questioned; Carr et al. (1979) note that there is no correlation between K_2O content and the depth of seismic focus in Central America. However, this observation only concerns recent lavas and does not take into account an evolution in time.

ACKNOWLEDGMENTS

REFERENCES

Aubouin, J., von Huene, R., Baltuck, M., Arnolt, R., Bourgois, J., Filewicz, M., Kvenvolden, K., Leinert, B., McDonald, T., McDougall, K., Ogawa, Y., Taylor, E., and Winsborough, B., 1982. Leg 84 of the Deep Sea Drilling Project; subduction without accretion: Middle America Trench off Guatemala. *Nature*, 297:458–460.

Aubouin, J., von Huene, R., et al., 1982. *Init. Repts. DSDP*, 67: Washington (U.S. Govt. Printing Office).

Bardintzeff, J. M., Brousse, R., Clochiatti, R., Weiss, J., 1980. Evolution des phénocristaux et de leurs inclusions magmatiques dans la "dacite" du dôme du Santiaguito (Guatemala). *C.R Acad. Sci. Paris*, 290(D):743–746.

Bellon, H., and Tournon, J., 1978. Contribution de la géochronométrie K-Ar à l'étude du magmatisme de Costa Rica, Amérique Centrale. *Bull. Soc. Géol. France*, 7(XX No. 6):955–959.

Boyles, F. A., Jack, R. N., and Carmichael, I. S. E., 1973. Investigation of deep-sea volcanic ash layers from equatorial Pacific cores. *Geol. Soc. Am. Bull.*, 84:2371–2388.

Cadet, J. P., Pouclet, A., Thisse, Y., Bardintzeff, J. M., and Azéma, J., 1982. Middle America Neogene explosive volcanism and ash layers: evidence from the Middle America Trench transect, *In* Aubouin, J., von Huene, R., et al., *Init. Repts. DSDP*, 67: Washington (U.S. Govt. Printing Office), 475–491.

Cadet, J. P., Thisse, Y., Pouclet, A., Bardintzeff, J. M., and Stephan, J. F., 1981. Tephra from Deep Sea Drilling Project Leg 66: Middle

America Trench transect (southern Mexico). *In* Watkins, J. S., Moore, J. C., et al., *Init. Repts. DSDP*, 66: Washington (U.S. Govt. Printing Office), 687–698.

Carey, S. N., and Sigurdsson, H., 1980. The Roseau ash: deep-sea tephra deposits from a major eruption on Dominica, Lesser Antilles Arc. *J. Volcanol. Geotherm. Res.*, 7(1–2):67–86.

Carr, M. J., Rose, W. I., and Mayfield, D. G., 1979. Potassium content of lavas and depth of the seismic zone in Central America. *J. Volcanol. Geotherm. Res.*, 5:387–401.

Drexler, J. W., Rose, W. I., Sparks, R. S. J., and Ledbetter, M. T., 1980. The Los Chocoyos ash, Guatemala: a major stratigraphic marker in Middle America and in three ocean basins. *Quat. Res.*, 13:327–345.

Irvine, T. N., and Baragar, W. R. A., 1971. A guide to the chemical classification of the common volcanic rocks. *Can. J. Earth Sci.*, 8: 523–548.

Keith, S. B., 1982. Paleoconvergence rates determined from K_2O-SiO_2 ratio in magmatic rocks and their application to Cretaceous and Tertiary tectonic patterns in southwestern North America. *Geol. Soc. Am. Bull.*, 93:524–532.

Kuno, H., 1968. Differentiation of basalt magmas. *In* Hess, H. H., and Poldervaart, A. (Eds.), *Basalts* (Vol. 2): New York (Interscience, Wiley), 623–688.

Lonsdale, P., and Klitgord, K. D., 1978. Structure and tectonic history of the Eastern Panama basin. *Geol. Soc. Am. Bull.*, 89:981–999.

Molnar, P., and Sykes, L. R., 1969. Tectonics of the Caribbean and Middle America regions from focal mechanisms and seismicity. *Geol. Soc. Am. Bull.*, 80:1639–1684.

Pecerillo, A., and Taylor, S. R., 1976. Geochemistry of Eocene calc-alkaline volcanic rocks from the Kastamonu area, Northern Turkey. *Contrib. Mineral. Petrol.*, 58:63–81.

Robock, A., and Matson, M., 1983. Circum-global transport of the El Chichon volcanic dust cloud. *Science*, 221:195–197.

Romeder, J. M., 1973. *Méthodes et Programmes d'Analyse Discriminante:* Paris (Bordas Dunod Ed.).

Rose, W. I., 1972a. Santiaguito volcanic dome, Guatemala. *Geol. Soc. Am. Bull.*, 83:1413–1434.

_____, 1972b. Notes on the 1902 eruption of Santa Maria volcano, Guatemala. *Bull. Volcanol.*, 36:29–45.

Rose, W. I., Jr., Anderson, A. T., Woodruff, L. G., and Bonis, S. B., 1978. The October 1974 basaltic tephra from Fuego volcano; description and history of the magma body. *J. Volcanol. Geotherm. Res.*, 4:3–53.

Rose, W. I., Jr., Bornhorst, T. J., and Drexler, J. W., 1982. Preliminary correlation of Quaternary volcanic ashes from the Middle America Trench off Guatemala, Deep Sea Drilling Project leg 67. *In* Aubouin, J., von Huene, R., et al., *Init. Repts. DSDP*, 67: Washington (U.S. Govt. Printing Office), 493–495.

Rose, W. I., Jr., Hahn, G. A., Drexler, J. W., Malinconico, M. L., Peterson, P. S., and Wunderman, R. L., 1981. Quaternary tephra of Northern Central America. *In* Self, S., and Sparks, R. S. J. (Eds.), *Tephra Studies:* Holland (D. Riedel Publ. Co.), pp. 193–211.

Schmincke, H. U., 1983. Rhyolitic and basaltic ashes from the Galapagos mounds area, Leg 70, Deep Sea Drilling Project. *In* Cann, J. R., Langseth, M. G., Honorez, J., Von Herzen, R. P., White, S. M., et al., *Init. Repts. DSDP*, 69: Washington (U.S. Govt. Printing Office), 451–457.

Woodruff, L. E., Rose, W. I., and Rigot, W., 1979. Contrasting fractionation patterns for sequential magmas from two calc-alkaline volcanoes in Central America. *J. Volcanol. Geotherm. Res.*, 6: 217–240.